Materials for Energy
Workshop "Advances in Fuel Cells and Hydrogen"
April 2010, Torres Vedras, Portugal

POLARITY REVERSAL BY FUEL STARVATION IN PEM FUEL CELLS

M.A. TRAVASSOS*, C.M.RANGEL*

LNEG – Laboratório Nacional de Energia e Geologia, Fuel Cells and Hydrogen Unit,
Estrada do Paço do Lumiar, 22 1649-038 Lisboa Portugal
*antonia.travassos@lneg.pt; *carmen.rangel@lneg.pt

ABSTRACT: In this work, the degradation caused by polarity reversal by fuel starvation of a 16 MEA (membrane-electrode assembly) – low power PEM fuel cell is reported. Measuring of the potential of individual cells, while on load, was found instrumental in the location of affected cells which revealed very low or even negative potential. *Ex-situ* analysis of MEA, after irreversible degradation by fuel starvation, gave as a result delamination of catalyst layers with impacts on fuel cell performance such as development of flooded areas (in the created gaps by membrane separation) increasing the resistance of reactant transport to the catalyst sites. Striking thickness variations of the anode layers as well as carbon corrosion were found. Also, the proton exchange membrane was found to be affected by fluoride depletion.

Keywords: polarity reversal, fuel starvation, PEM degradation.

RESUMO: Neste trabalho, relatam-se as causas da degradação de uma célula de combustível PEM de baixa potência constituída por 16 MEAs (conjunto membrana-eléctrodo), devido à inversão de polaridade por privação de combustível. A medição individual do potencial das células, em condições de demanda de corrente, revelou que as células afectadas apresentam valores de potencial muito baixos e até negativos.
Uma análise *ex-situ* da MEA, após ocorrência de degradação irreversível por privação de combustível, resultou em delaminação de camadas de catalisador com impacto sobre o desempenho de célula de combustível dando lugar ao desenvolvimento de áreas inundadas aumentando a resistência ao transporte de combustível para os sítios activos no catalisador. A variação da espessura da camada catalítica anódica é expressiva bem como a corrosão de carbono. A membrana de troca de protões é afectada por depleção de fluoreto.

Palavras chave: inversão de polaridade, privação de combustível, degradação da PEM.

1. INTRODUCTION

The reliability and cost together with the durability are paramount to the implementation of fuel cells as alternative energy conversion devices. Durability criteria for fuel cells require a minimum lifetime of 40 000 hours for stationary applications and 5 000 hours for automotive applications [1, 2], making materials degradation a critical issue and creating the need for a more comprehensive knowledge about the mechanisms which are, at the present, not well understood.

Fuel cells are prone to chemical, mechanical or thermal degradation modes that lead to a voltage/performance decline and lifetime reduction. Fuel cell design and assembly, materials properties, operational conditions and the tolerance to impurity or contaminants are within the recognized degradation causes.

The major possible failure causes identified for the membrane-electrode assembly (MEA) are cracking, delamination, catalyst clusterization and thickness variations, which may occur due to manufacturing or operating conditions.

Also, PEM fuel cells lifetime can be reduced by chemical degradation of the MEA, Pt dissolution and/or agglomeration or carbon corrosion promoted by MEA contamination and power or thermal cycling.

The baseline degradation is irreversible and unavoidable, due to long-term materials degradation in the context of load cycling and/or the influence of the variation of operating conditions, such as temperature and humidity, on cell performance.

Degradation and failure also occurs under less controllable conditions such as reactant starvation, particularly fuel starvation [2-7].

The corrosion of the catalyst carbon support in a PEMFC interferes with the performance and lifetime of the MEA. Carbon corrosion occurs supported by operational conditions such as absence of fuel or fuel starvation.

Platinum (Pt), the most common material used as catalyst in PEM fuel cells, is usually supported on carbon in the form of nano-dispersed particles. Carbon is an excellent material for supporting electrocatalysts, allowing facile mass transport of reactants and fuel cell reaction products besides good electrical conductivity and stability under normal conditions. Nevertheless the instability of carbon under PEMFC conditions promote breakdown in the fuel cell performance with oxidation of carbon into carbon dioxide. Oxidation of carbon support, referred as carbon corrosion, leads to an accelerated loss of active surface area and alteration of pore morphology. The deactivation of active catalyst is due to CO formed by CO_2 reduction [5, 6].

In a fuel cell stack, when some cells are in starvation, potential will drop to a lower level. If the starvation is not too severe and the reactants are enough to maintain the stack current, the voltage of these cells will be positive though lower than others. However when the fluxes of reactants are not enough to maintain the stack current, to balance the current value, there must be a part of the electrolysis current which will make the voltage of the starved cells drop to negative. This process is named cell reversal or polarity reversal.

The starved cells are driven into reversed operation with the cell potential negative and the cell works in an electrolysis mode which damages the electrodes.

In the carbon corrosion process the catalyst support is converted to CO_2 and in addition the Pt or Pt/Ru particles may be lost from the electrode with missing performance.

In this work, polarity reversal caused by fuel starvation of a 16 MEA low power fuel cell is reported associated to an application in emergency exit lighting. Morphological defects detected by SEM/EDS were linked to delamination and thickness variation.

2. EXPERIMENTAL

In this work an emergency exit light which integrated a NiCd battery of 3.6V with storage capacity of 4Ah, was substituted by a low power PEM fuel cell supplied with hydrogen.

Emergency exit lightening is usually associated to big capacity batteries or a modest autonomy. In this case the system with hydrogen fuel cells can extend the system autonomy and give others advantage such as easier logistic when compared to battery maintenance.

The fuel cell, SRE technology, had a nominal power of 15 W (16 cells) and the metallic hydride small reactor had a capacity for 50 NL H_2.

The PEM fuel cell performance was studied allowing evaluation of the fuel cell autonomy.

While on loading, the fuel cell was operated during one hour daily. Measurements of cell potential took place every 15 minutes. The potential was registered for every of the 16 cells integrating the stack.

The MEA morphological aspects, after failure and dismantling of the cell, were observed by SEM/EDS. Elemental mapping was implemented for MEA cross section analysis in order to register the elemental chemical distribution of P, F and S.

Figure 1 shows the schematic drawing of the PEM fuel cell (A) used in this work as well as the circuit implemented using a hydrogen storage system constituted by a metallic hydride (B).

(A)

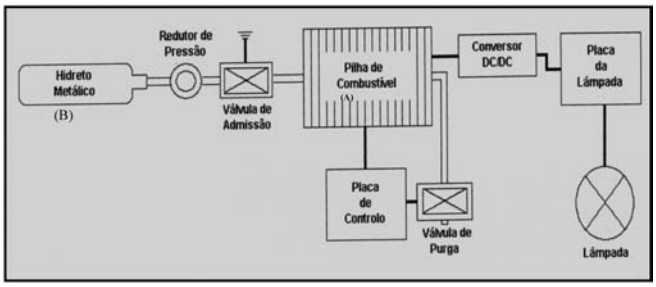

Fig. 1. PEMFC and an electrical circuit feeding an emergency exit lightening with a H_2 fuel cell (A). Metallic hydride (B) as hydrogen storage system.

3. RESULTS

While on load, emergency light switched-on, the cell potential values were individually measured showing a dependency on cell position in the stack. Lower values are reported for the farthest cells from hydrogen entry. The potentials values varied from 0.653V down to 0.492V. Figure 2 shows the evolution of the potential with time, with the lowest values associated to cells 15 and 16.

Data registered for 3 consecutive days were very similar, with a slight increase in potential values.

With continuous operation using a reduced hydrogen flow an inversion of polarity was observed in the 16th cell of the stack, evident in the potential vs. time plot in figure 3, as a result of insufficient hydrogen to reach the last cells.

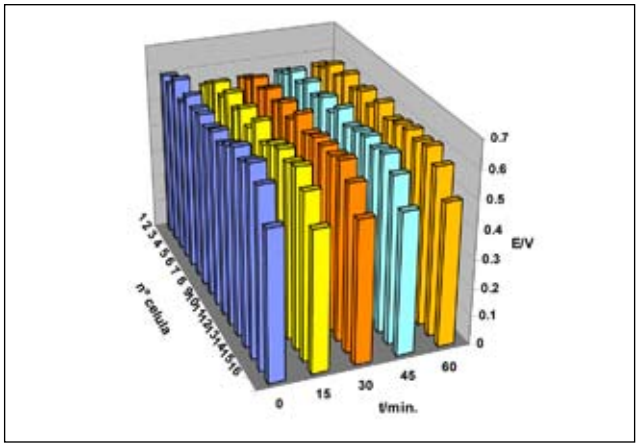

Fig. 2. Cell potential *versus* time for a 15 W fuel cell stack of 16 cells. Data are referred to one hour operation, with measurements every 15 minutes.

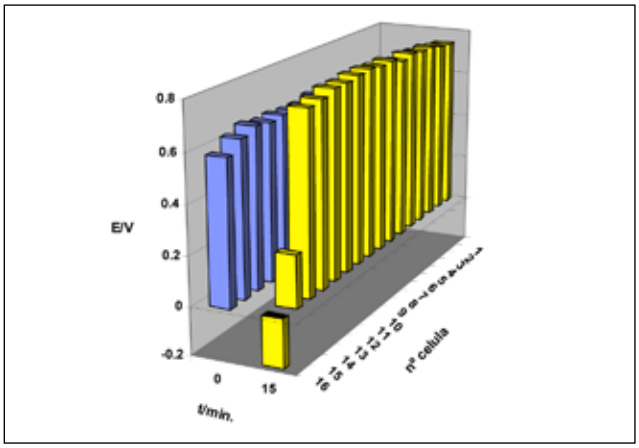

Fig. 3. Cell potential of a 16 cell low power PEM fuel cell *versus* working time showing polarity reversal in cell 16 and potential below 0.2 V in cell 15.

The degradation level of the fuel cell was evaluated by measuring the potential with time every 30 minutes, figure 4, being more accentuated the difference between the potential of the middle cells in comparison with the peripheral cells that presented lowers values, particularly the 16th cell.

Once the phenomenon is made irreversible, the cell was dismantling in order to observe the degradation of the MEA.

The cells were observed under the SEM after cross section mounting. Images revealed the presence of morphological defects associated to fuel starvation.

The SEM observation of the cross sections was accompanied by EDS mapping for Pt, S and F, corresponding to the 16th cell. Results are represented in figure 5. The images show delamination at the anode and a striking difference of thickness when compared to the cathode catalyst layer (C), see table 1.

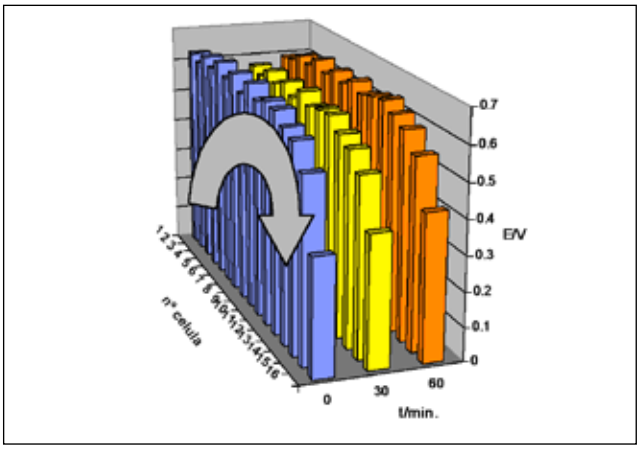

Fig. 4. Cell potential of a 16 cell low power PEM fuel cell after polarity reversal, when the full flux of hydrogen was replenished.

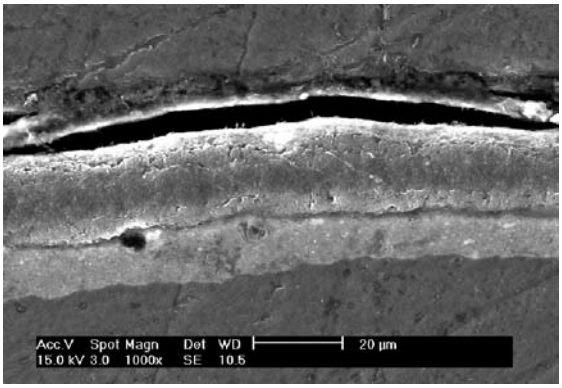

(a)

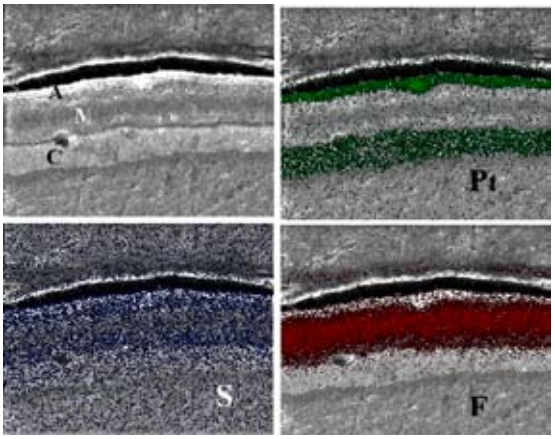

(b)

Fig. 5. SEM image of cross section of the MEA of the 16th cell showing delamination (a) and the results of elemental mapping for the Pt, S and F. A= anode; C= cathode and M= membrane (b).

Table 1. Anode, cathode and membrane average thicknesses of different cells in the tested PEM stack.

Sample	Anode Thickness µm	Cathode Thickness µm	Membrane Thickness µm
Cell 1	10.02	9.79	14.21
Cell 9	10.63	9.98	18.63
Cell 16	4.86	12.96	17.74

4. DISCUSSION

It is noticed that in presence of fuel starvation, cell voltage can become negative. The anode achieves positive potentials and at same time the carbon is consumed [3,7]. The diagram, figure 6, describes the typical time-dependent change of the cell terminal voltage. It is observed that the cell voltage drops suddenly to negative values and the MEA changes polarity due to the cell reversal. The cell terminal voltage reveals an initial drastic drop reaching a steady decrease with time. The reversal cell polarity occurred when the anode potential increased and became more positive than cathode potential.

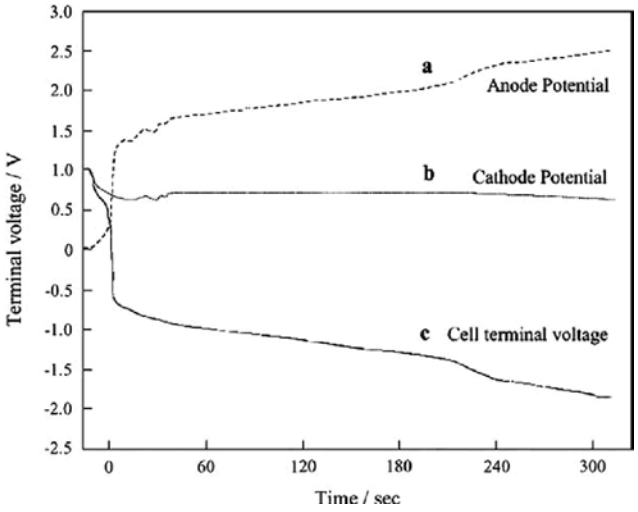

Fig. 6. Time-dependent changes in anode (a), cathode (b) and cell potential (c) during a cell reversal experiment [3].

The anode potential increase until water electrolysis occurs (near 1.5V), figure 7, according reaction (1).

In absence of fuel or in presence of fuel starvation on the anode side state entails water electrolysis and carbon oxidation (carbon corrosion) at the fuel cell anode in order to the required protons and electrons for the oxygen reduction reaction happening at the cathode, with the following reactions:

Water electrolysis: $2H_2O \rightarrow O_2 + 4H^+ + 4e^-$ (1)

Carbon corrosion: $C + 2H_2O \rightarrow CO_2 + 4H^+ + 4e^-$ (2)

The water electrolysis plateau in the figure 7 is due to the reaction (1), confirmed by the high current efficiency for oxygen evolution. At high anode potential a small degree of carbon corrosion, reaction (2), accompanies water electrolysis as shown in the figure 7 by the small amount of CO_2 detected. The figure exhibits a carbon corrosion plateau as the cell potential reaches -1.4V. At this stage the current is increased by carbon corrosion rather than by water electrolysis [8-11].

Most current technology development is focused on the use of Pt (or PtRu) supported on carbon particles in order to reduce amount of Pt required. Carbon oxidation weakens the attachment of Pt particles to the carbon support and eventually leads to a structural collapse and detachment from the carbon surface. As carbon corrodes away catalyst nanoparticles will be lost from the catalyst layer and either aggregate in to larger particles or migrate to the polymer electrolyte . This is shown schematically in Figure 8.

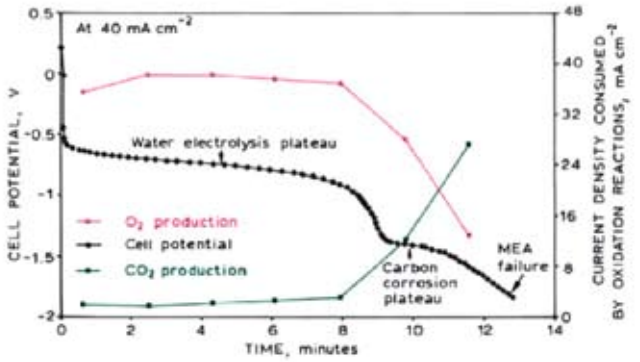

Fig. 7. The change in the cell potential at 40 mA cm^{-2} and the rate of oxygen and CO_2 produced at an MEA during cell reversal due to fuel starvation [9].

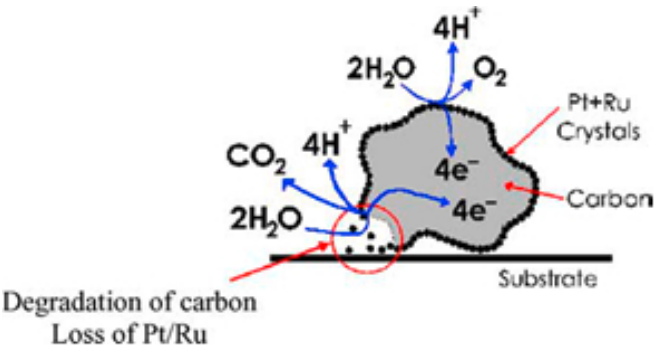

Fig. 8. Schematic representation of degradation of carbon catalyst support during operation in the absence of fuel [12].

In this work the following observations sustained evidence for polarity reversal failure caused by insufficient hydrogen:

The 16th cell presented the lowest performance and also the greater reduction on the anode thickness compared with the other cells, this is thought to be due to the consequences of polarity reversal.

The thickness variations can promote variable resistance through the MEAs. Thicker areas of the catalyst layer will have higher electronic resistance, while thicker electrolyte segments will have increased ionic resistance. For thinner areas, the opposite will be true. The thinner areas of the ionomer coupled with a thicker catalyst layer will be more susceptible to degradation by heat.

Since the mechanical strength of the MEA comes partially from the electrolyte membrane, areas where the electrolyte is deep-set by the catalyst layer may be mechanically weak and thus may tear easily with tension. This may cause problems with pressure differentials and mechanical stress during thermal and hydration cycles [1].

The first cell presents also delamination with separation between catalyst layer (anode A) and polymer membrane electrolyte (M).

The delamination can also increase resistance in the MEAs. The separation of the catalyst layer from the electrolyte reduces also the total contact area between the two layers. Hence,

the contact resistance between the materials will increase, the protons will have a longer path to travel to catalyst sites, and the water barrier will be more resistive to proton conduction than pure electrolyte.

Some morphological features observed were adjudicated to carbon corrosion.

Fluoride depletion in the membrane is suggested near the borderline with the catalyst layer on both anode and cathode side, this is clearly observed in figure 5 after elemental mapping of fluoride in the MEA cross section.

Cells located in the middle of the stack are more homogeneous and show no delamination.

5. FINAL REMARKS

Polarity reversal, caused by fuel starvation, was identified as the main cause of failure of a 16 MEA low power PEM fuel cell. The fuel cell was associated to an emergency exit lighting application in which a conventional battery was substituted by a fuel cell.

It was verified that the measurement of individual cell potentials was instrumental in the monitoring of cell reversal with lower values been reported for the farthest cell from hydrogen entry.

Morphological aspects revealed by SEM/EDS analysis were linked to delamination and thickness variation of the anode catalyst layer.

Carbon corrosion and fluoride depletion in the membrane were also evident contributing to irreversible damage of the MEA.

REFERENCES

[1] S. Kundu, M.W. Fowler, L.C. Simon, S. Grot, *J. Power Sources,* 157 (2006) 650-656.

[2] N. Yousfi-Steiner, Ph. Moçotéguy, D. Candusso, D. Hissel, *J. Power Sources,* 194 (2009) 130-145.

[3] A. Taniguchi, T. Akita, K. Yasuda, Y. Miyazaki, *J. Power Sources,* 130 (2004) 42-49.

[4] Z. Liu, L. Yang, Z. Mao, W. Zhuge, Y Zhang L. Wang, *J. Power Sources,* 157 (2006) 166-176.

[5] G. J. M. Janssen, *J. Power Sources,* 136 (2004) 45-54.

[6] S. Maass, F. Finsterwalder, G. Frank, R. Hartmann, C. Merten, *J. Power Sources,* 176 (2008) 444-451.

[7] J. Wu, X. Z. Yuan, H. Wang, M. Blanco, J. J. Martin and J. Zhang, *Int. J. Hydrogen Energy*, 33 (2008) 1735--1746.

[8] R. Borup J. Meyers, B. Pivovar, Y.S. Kim, R. Mukundan, N. Garland, D. Myers, M. Wilson, F. Garzon, D. Wood, P. Zelenay, K. More, K. Stroh, T. Zawodzinski, J. Boncella, J.E. McGrath, M. Inaba, K. Miyatake, M. Hori, K. Ota, Z. Ogumi, S. Miyata, A. Nishikata, Z. Siroma, Y. Uchimoto, K. Yasuda, K.-I. Kimijima, N. Iwashita, *Chem. Rev*. 107 (2007) 3904-3951.

[9] T. R. Ralph and M.P. Hogarth, *Platinum Met. Rev*. 46 (2002) 117-135.

[10] S. Zhang, X. Yuan, H. Wang, W. Mérida, H. Zhu, J. Shen, S. Wu, J. Zhang, *Int. J. Hydrogen Energy*, 34 (2009) 388-404.

[11] Yi Yu, Z. Tu, H. Zhang, Z. Zhan, M. Pan, *J. Power Sources,* 196 (2011) 5077-5083.

[12] S. D. Knights, K. M. Colbow J. St-Pierre, D. P. Wilkinson, *J. Power Sources,* 127 (2004) 127-134.